stellarator news

Published by Fusion Energy Division, Oak Ridge National Laboratory
Building 5700 P.O. Box 2008 Oak Ridge, TN 37831-6169, USA

Editor: James A. Rome Issue 90 January 2004
E-Mail: jar@ornl.gov Phone (865) 482-5643
On the Web at http://www.ornl.gov/sci/fed/stelnews

# Evidence of a toroidally symmetric, poloidally asymmetric radiation feature in the final stage of thermal collapse of the LHD plasma

## 1. Introduction

Plasma density is one of three major plasma parameters contributing to the fusion triple product, which is a figure of merit for a fusion reactor. In tokamaks the density is typically limited by a current disruption near the Greenwald density [1]. Helical devices, in which the magnetic field is independent of the plasma current, can avoid these disruptions. The main mechanism of density limitation in a helical device is a thermal instability. This instability is initiated when the plasma temperature drops and the edge temperature reaches a critical point at which the radiation from light impurities at the plasma edge grows with decreasing temperature; this results in a positive feedback loop because the radiation cools the plasma further. This type of mechanism was first observed and also appears in tokamaks [2], but only in "dirty" plasmas with large impurity concentrations. In "clean" tokamak plasmas, this density limitation is precluded by the current disruption (Greenwald) limit.

The empirical scaling of the density limit for helical systems is given by Sudo [3] as proportional to the square root of the product of input power and magnetic field strength divided by the plasma volume, $\sim(PB/V)^{0.5}$. Therefore, in helical systems the maximum achievable density increases as the square root of the input power, whereas in tokamaks it is a very weak function of input power. Hence, in terms of the density limit, helical devices have a strong advantage over tokamaks. Extensive studies of the density limit in the W7-AS stellarator show a scaling similar to that of Sudo [4]. Studies of the density limit in the Large Helical Device (LHD) have focused on the asymmetric radiation observed in the final stages of the discharge [5,6] and the evolution of the collapse in comparison with discharges that are terminated at lower density when the neutral beam is turned off [7].

Here we add to this research new information from bolometer diagnostics on the three-dimensional (3D) structure of the radiative collapse. In Section 2 the evolution of the radiative collapse is reviewed. In Section 3 we discuss the 3D structure of the radiative collapse, drawing on data from various diagnostics and particularly on the comparison of bolometer images with model reconstructions. In Section 4 the report is summarized and the overall results are discussed.

## 2. Evolution of radiative collapse

LHD is the world's largest helical experiment and uses the world's largest superconducting coil system to produce the steady-state confining magnetic field [8]. The ports in LHD are numbered one through ten, corresponding to the ten toroidal field periods of the device. Integral numbers refer to the horizontally elongated cross sections, and vertically elongated cross sections are indicated by halves. The plasma is typically heated by neutral beam injection

## *In this issue . . .*

after initiation by microwaves. The radiative collapse evolves in three steps, indicated in Fig. 1.

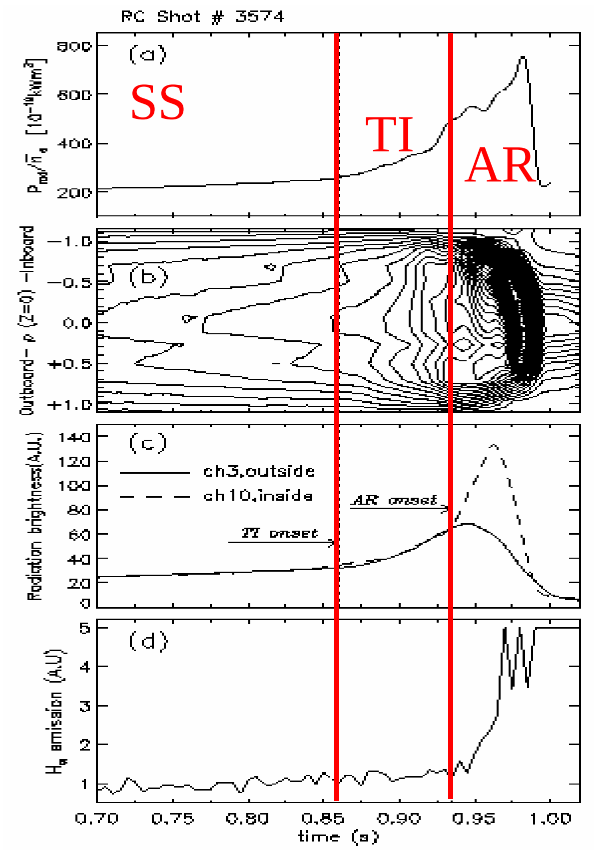


**Fig. 1.** Evolution of radiative collapse in LHD. (a) The ratio of the total radiated power to the line-averaged electron density, (b) radiated power brightness profiles at the vertically elongated plasma cross section, observed at Port 6.5, (c) signals from inboard and outboard bolometer channels of the bolometer at Port 6.5, and (d) the $H_\alpha$ signal.

The first phase is the steady-state (SS) phase in which the radiated power increases almost as a constant fraction of the density [Fig. 1(a)]. The collapse begins with the initiation of the thermal instability (TI) phase, when the radiated power begins to increase much more quickly than the density, indicating that the cooling rate is increasing (if the impurity density is constant). This is followed by the asymmetric radiation (AR) phase, which is evident in the bolometer brightness profile evolution at the vertically elongated cross section [9] in Fig. 1(b) and in the comparison of signals from inboard and outboard bolometer chords in Fig. 1(c). In addition to the asymmetry in the radiation, a concurrent asymmetry is observed in the electron density [5] and temperature profiles [7], which is similar to what is observed during the MARFE phenomenon in tokamaks [5, 10].

## 3. 3D structure of the asymmetry

In addition to the asymmetries observed in the bolometer profiles in Fig. 1 from Port 6.5, numerous other diagnostics can provide clues as to the 3D structure of the asymmetry. As mentioned in Section 2, an asymmetry is observed in the electron temperature profile measured by the Thomson scattering diagnostic at a horizontally elongated cross section at Port 4 [7]. These data show a low-temperature region below 20 eV at the inboard side of the profile, while the electron temperature at the outboard side was around 50 eV during the AR phase. In addition, the electron density measured at the vertically elongated cross section at Port 8.5 with a far infrared (FIR) interferometer shows an asymmetry with higher density at the inboard side. This results in a degradation of the signal, which is temporally and spatially (at a similar radial position, two field periods away) coincident with the asymmetry in the bolometer signal shown in Fig. 1(b) [5].

In addition to these data, numerous bolometric diagnostics [9] provide information on the 3D structure of the asymmetry. Besides the array at the vertically elongated cross section whose data is shown in Fig. 1, another resistive bolometer array fanning out vertically is installed viewing the horizontally elongated cross section at Port 8. These data show a symmetric profile during the asymmetric phase indicating that there is no up-down asymmetry at this cross section [5]. Due to the orientation of this array it gives no information regarding the existence or nature of an asymmetry in the horizontal (major radial) direction. In addition to these resistive bolometers, two infrared (IR) imaging video bolometers (IRVBs) are installed, one with a top view of the plasma at Port 6.5 and one with a tangential view from a port located between Ports 5 and 6 and looking towards Port 6. The fields of view of these IRVBs are shown in Fig. 2.

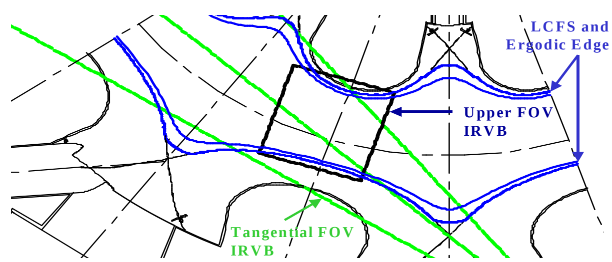


Fig. 2. Top view of LHD showing the last closed flux surface (LCFS) and ergodic edge (blue) with fields of view of IRVBs at Port 6.5 (black) and a tangential port (green).

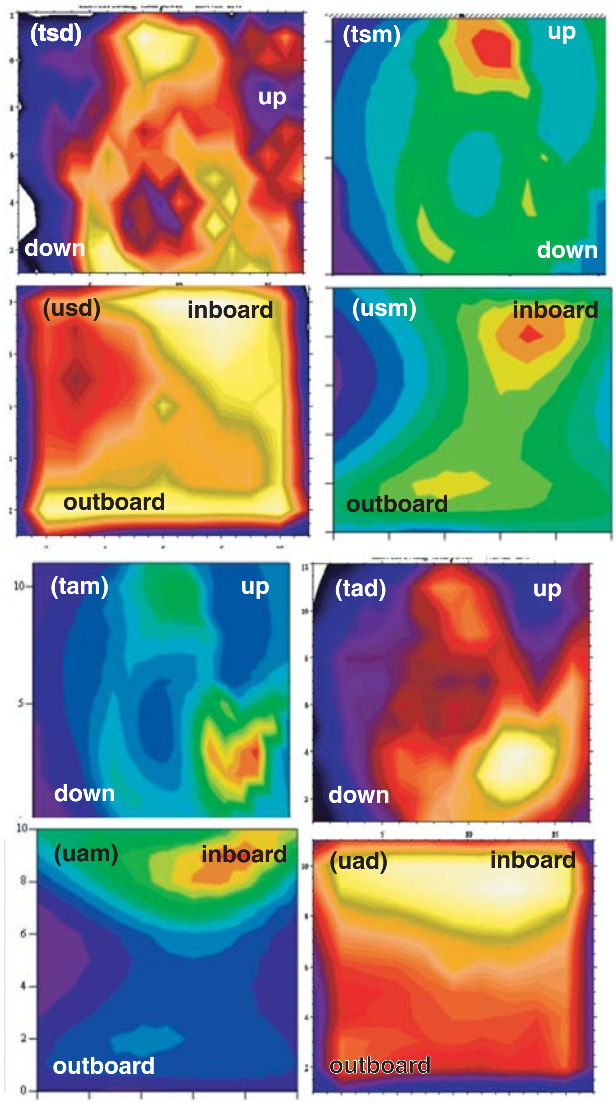


**Fig. 3.** IRVB radiation brightness image data (d) from upper (u) and tangential (t) ports during the steady-state (s) and asymmetric (a) phases of the discharge compared with reconstructions from model (m) profiles.

In Fig. 3 data from these IRVBs are shown and compared with model reconstructions. For the steady-state portion of the discharge, one notes fairly good agreement between the data and the reconstructions based on the poloidally and toroidally symmetric profile given by the hollow radiation density profile, $S(\rho)$, shown in Fig. 4, where $\rho$ is the normalized minor radius. Comparing the images from the symmetric phase to those of the asymmetric phase shows a region of intense radiation on the inboard side slightly below the horizontal midplane [6]. In the case of the asymmetric phase, the model is modified by adding a poloidally asymmetric term, $F(\theta)$, given by

$$S(\rho, \theta) = S(\rho)[1 + F(\theta)]$$

and

$$F(\theta) = \{[1 + \cos(\theta + 150)]/2\}^{50}$$

where $\theta$ is the poloidal angle. This gives good qualitative agreement with the experimental data, indicating that within the fields of view of these two imaging bolometers this phenomenon appears axisymmetric.

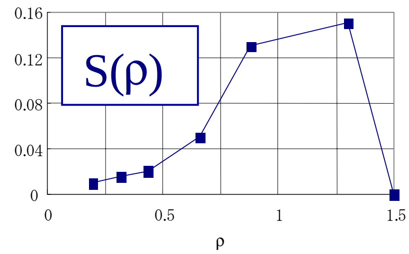


**Fig. 4.** Model radial profile of radiation density, $S(\rho)$ (a.u.).

Additional information on the two-dimensional location of this highly radiating region is given by the data in Fig. 5 from a tomographic analysis of data from two 20-channel arrays which view a semitangential plane between Ports 3 and 4 [9,11]. This shows that the highly radiating region is located at the inboard side near the horizontal midplane.

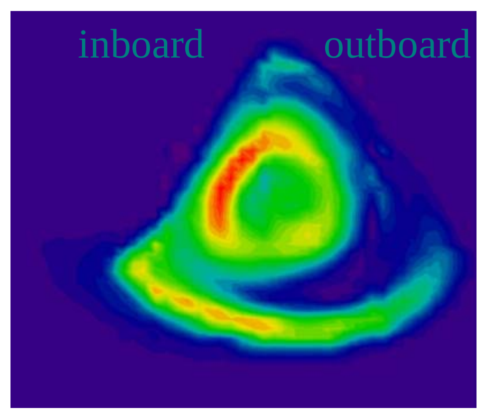


**Fig. 5.** Tomographic reconstruction of the absolute X-ray ultraviolet diode (AXUVD) data for the same shot and timing shown in Fig. 3 (a).

## 5. Summary and discussion

The achievable density in LHD is limited by radiative collapse preceded by a thermal instability in the light impurities. This thermal instability terminates in a poloidally asymmetric radiative collapse, which has many features in common with the MARFE phenomenon in tokamaks. Considering the 3D nature of the LHD vacuum vessel and magnetic field structure, one surprising feature which this asymmetric collapse has in common with a MARFE is axisymmetry. This is evident from seven different diagnostics, which cover the toroidal field periods from 3–4 and

6–8. While this asymmetry appears late in the collapse, we presume that it exists earlier in the process in the form of a poloidal asymmetry in the perpendicular thermal conductivity that is not evident until the edge temperature drops below a critical level [7]. Therefore, we think that this asymmetry may be playing an important role in the collapse and limitation of the density. We have recently added another imaging bolometer, which will enable us to investigate this phenomenon from field periods 5–7 and will enable 3D tomography of this phenomenon.

B. J. Peterson, N. Ashikawa, A. Yu. Kostrioukov,[1] Yi Liu,[2] and the LHD team
National Institute for Fusion Science, Toki, Japan 509-5292
[1]St. Petersburg Technical University, St. Petersburg, Russia
[2]Southwest Institute for Physics, Chengdu, China

### References

[1] M. Greenwald, Plasma Phys. Controlled Fusion **44** (2002) R27.

[2] N. Ohyabu, Nucl. Fusion **9** (1979) 1491.

[3] S. Sudo et al., Nucl. Fusion **30** (1990) 11.

[4] L. Giannone et al., Plasma Phys. Controlled Fusion **42** (2000) 603.

[5] B.J. Peterson et al., Phys. Plasmas **8** (2001) 3861.

[6] N. Ashikawa et al., J. Nucl. Mater. **313–316** (2003) 1103.

[7] Y. Xu et al., Nucl. Fusion **42** (2002) 601.

[8] A. Komori et al., Plasma Phys. Controlled Fusion **45** (2003) 671.

[9] B.J. Peterson et al., Plasma Phys. Controlled Fusion **45** (2003) 1167.

[10] B. Lipschultz et al., Nucl. Fusion **24** (1984) 977.

[11] Y. Liu et al., Rev. Sci. Instrum. **74** (2003) 2312.

# Extended abstracts

## Experimental check of neoclassical predictions for the radial electric field in a stellarator

Nucl. Fusion **43** (2003) L11–L13

Investigations of the radial electric field have been carried out at the stellarator Wendelstein 7-AS using charge-exchange spectroscopy (CXS) with high spatial resolution based on the high-energy lithium beam diagnostic (Li-CXS). To evaluate the electric field, the radial force balance equation is used together with the measured profiles of poloidal velocity, density and temperature of carbon impurities. Results of experiments are compared with predictions of the neoclassical theory. We also use a simple analytic approximation, in which the radial electric field is proportional to the pressure gradient of $H^+$ ions of the bulk plasma. This approximation quite reasonably agrees with both the measurements and the accurate neoclassical calculations and, as shown in Fig. 1, can therefore be used for a fast estimation of the radial electric field.

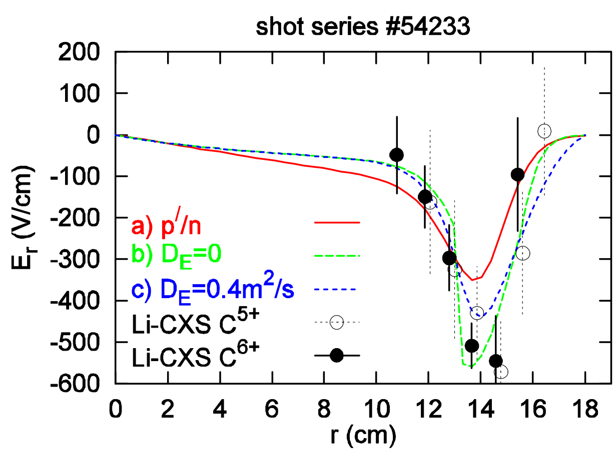


**Fig. 1.** Radial electric field measured by the Li-CXS diagnostic (symbols). The data of $C6^+$ have higher accuracy. Results from neoclassical theory: (a) the approximation proportional to the pressure gradient; (b) the solution of the algebraic ambipolarity constraint; (c) the solution of a diffusion equation for the radial electric field based on a thermodynamic approach. The diffusivity originates from the plasma viscosity.

H. Ehmler, Y. Turkin, C. D. Beidler, H. Maassberg, A. Dinklage, T. Klinger, and the W7-AS Team

## Doppler reflectometry with optimized temporal resolution for the measurement of turbulence and its propagation velocity

Submitted to Plasma Physics and Controlled Fusion

M. Hirsch, E. Holzhauer
Max-Planck-Institut für Plasmaphysik
Teilinstitut Greifswald
Wendelsteinstraße 1
D-17491 Greifswald
Germany

Doppler reflectometry selects electron density perturbations with finite wave vector $K_\perp$ by a line of sight which is nonperpendicular with respect to the reflecting layer. This provides simultaneously a local measurement of the propagation velocity of these perturbations $v_\perp(K_\perp)$ and of changes in their fluctuation amplitude $\tilde{n}(K_\perp)$ [1]. A quantitative measurement of $v_\perp$ with a temporal resolution sufficient to study the dynamics between $\nabla v_\perp$ and the $K_\perp$-spectrum of turbulence requires an optimization of the antenna characteristic and of the geometry between the antenna and reflecting layer. Reduced plasma curvature, which it is available at selected positions of stellarator configurations, improves the resolution in $K$-space of the turbulence and thus eases the separation of the selected diffraction order –1 from the unwanted strong 0th-order reflection used in conventional reflectometry. Therefore the multichannel Doppler reflectometer at W7-AS is installed at a toroidal plane with vertically elongated plasma that offers minimized curvature. In addition, the steep edge density gradients of W7-AS provide a high radial localization of the measurement.

The antenna system and signal detection of the Doppler reflectometer are optimized for maximum temporal resolution in order to study transport bifurcations such as the transition between L- and H-mode. Frequency spectra of the returning microwave and the quantities $v_\perp$ and $\tilde{n}$ are obtained by a 15-channel spectrum analyzer. The tilt angle of the antenna with respect to the normal onto the reflecting layer $\theta_{tilt} = 14°$ selects perturbations with poloidal wavelength $\Lambda_\perp \approx 0.8$ cm according to the Bragg condition. For example, Fig. 1 shows three spectra selected from a time window around an H- to L-mode back-transition which occurs after the neutral beam heating has been switched off. The individual filter bandwidths are indicated by horizontal bars. Note the log scale of the vertical axis. Each spectrum is integrated over $4\ \mu s$ and fitted to Gaussian line shapes as expected from the antenna characteristics. The spectrum measured in the H-mode (blue dots) shows high rotation (Doppler shift) and low turbulence level (displayed by the amplitude of the frequency shifted signal). At a time 4 ms prior to the back transition (green dots), rotation has already started to decrease and turbulence is increasing. The frequency shift of 3.7 MHz corresponds to $v_\perp = 27$ km/s. In the L-mode (red dots), the fluctuation level is increased by more than an order of magnitude and the propagation velocity of the turbulence is low. The radial position chosen by the microwave frequency (85 GHz) is located 2 cm inside the separatrix, which is about at the maximum $\boldsymbol{E} \times \boldsymbol{B}$ shear as measured from spectroscopy.

### Reference

[1] M. Hirsch, E. Holzhauer, J. Baldzuhn, B. Kurzan, and B. Scott 2001 Plasma Phys. Controlled Fusion **43** (2001)1641.

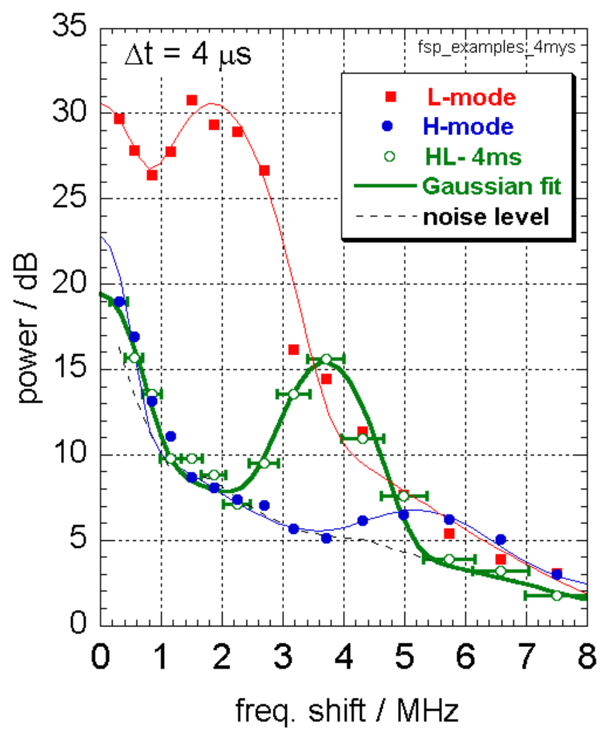


**Fig. 1.** Doppler reflectometer output at the time of an H- to L-mode back-transition.

# Meetings

## First Announcement of Joint Meeting of US-Japan Workshop and Kyoto University 21st COE Symposium on *New Approaches to Plasma Confinement Experiments in Helical Systems*

Dear Colleagues:

We are pleased to invite you to participate in the Joint Meeting of US-Japan Workshop and Kyoto University 21st Center of Excellence Symposium on *New approaches to plasma confinement experiments in helical systems* to be held at Kyoto University, Japan. the 21st Center of Excellence is supported by the Ministry of Education, Culture, Sports, Science, and Technology (MEXT, formerly MOE).

The meeting will be organized by the Institute of Advanced Energy of Kyoto University in the frame of the 2003 US–Japan Cooperation Programs in Fusion Physics and the Kyoto University 21st COE Program *Establishment of COE on Sustainable Energy System*. The meeting covers the topics and areas of new approaches to plasma confinement experiments in helical systems, especially, in advanced helical systems such as those with quasi-axial, quasi-helical, or quasi-poloidal symmetry, or quasi-omnigeneneity. Recent progress of the related experiments, theories, engineering and design studies will also be discussed. The program will consist of oral presentations. Further information is given below.

**Date of Meeting:** March 2–4, 2004

**Place:** The Institute of Advanced Energy, Kyoto University, Japan

### *1. Topics*

Recent experimental projects
Configuration optimization
Transport and confinement improvement
MHD equilibrium and stability
Turbulence and transport
Particle and power handling
Divertor and impurity control/transport
Plasma heating
Reactor studies
Engineering and design studies

### *2. Schedule*

Pre-registration: January 16, 2004
Deadline for one-page abstract (only electronic submission acceptable): February 1, 2004
Deadline for registration: February 13, 2004
Workshop at IAE, Kyoto University: March 2–4, 2004

### *3. Accommodations*

A block of rooms has been reserved for foreign participants at the New-Miyako Hotel, located just in front of Japanese Rail Kyoto Station. Those who wish to make reservations at the New-Miyako Hotel should contact the workshop secretary. The room rate at the New-Miyako Hotel is about 9,000 yen (tax and service charge are not included). Please see the workshop web site (http://www.center.iae.kyoto-u.ac.jp/plasma/usj04/index.html) for information about other hotels.

### *4. Key Persons*

F. Sano (Kyoto University)
D. T. Anderson (University of Wisconsin-Madison)

### *5. Workshop Secretary*

K. Nagasaki (Kyoto University)

Detailed information will be given in the second announcement on the web site. General correspondence concerning the workshop should be directed to the workshop secretary.

E-mail: nagasaki@iae.kyoto-u.ac.jp
Mail: K. Nagasaki, Dr.
Institute of Advanced Energy, Kyoto University
Gokasho, Uji, Kyoto 611-0011, Japan
Phone: +81-774-38-3530
Fax: +81-774-38-3535